Materials Science and Engineering C 33 (2013) 1876–1881

Contents lists available at SciVerse ScienceDirect

Materials Science and Engineering C

journal homepage: www.elsevier.com/locate/msec

Comparative study of carp otolith hardness: Lapillus and asteriscus

Dongni Ren [a], Marc André Meyers [c], Bo Zhou [d], Qingling Feng [b,*]

[a] State Key Laboratory of New Ceramics and Fine Processing, Department of Materials Science and Engineering, Tsinghua University, Beijing 100084, China
[b] Laboratory of Advanced Materials, Department of Materials Science and Engineering, Tsinghua University, Beijing 100084, People's Republic of China
[c] Materials Science and Engineering Program, Departments of Nanoengineering and Mechanical and Aerospace Engineering, University of California, San Diego, La Jolla, CA 92093, United States
[d] CSM Instruments Inc., 197 1st Avenue, Suite 120, Needham, MA 02494, United States

ARTICLE INFO

Article history:
Received 27 June 2012
Received in revised form 19 September 2012
Accepted 26 October 2012
Available online 2 November 2012

Keywords:
Otolith
Nano-indentation
Microhardness

ABSTRACT

Otoliths are calcium carbonate biominerals in the inner ear of vertebrates; they play a role in balance, movement, and sound perception. Two types of otoliths in freshwater carp are investigated using nano- and micro-indentation: asteriscus and lapillus. The hardness, modulus, and creep of asteriscus (vaterite crystals) and lapillus (aragonite crystals) are compared. The hardness and modulus of lapillus are higher than those of asteriscus both in nano- and micro-testing, which is attributed to the different crystal polymorphs. Both materials exhibit a certain degree of creep, which indicates some time dependence of the mechanical behavior and is attributed to the organic components. The nano-indentation hardnesses are higher than micro-hardnesses for both otoliths, a direct result of the scale dependence of strength; fewer flaws are encountered by the nano than by the microindenter.

1. Introduction

Otoliths are calcium carbonate structures in the inner ear of vertebrates. They have a function in balance, movement, and sound detection. They are located in the membrane labyrinth of the inner ear. There are three pairs of otoliths: lapillus, sagitta and asteriscus. They are located in the utriculus, sacculus and lagena of fish inner ear, respectively. In our previous work [1], it is established that the fresh water carp otoliths, lapillus and sagitta, are composed of pure aragonite crystals and organic matrices; the asteriscus is composed of pure vaterite crystals and organic matrix. The hierarchical structures of these otoliths were established [2,3]. The existence of different calcium carbonate polymorphs in a single organism, also in pure crystal phase state provides ideal research material for the study of biomineralization, such as the effect of organic mediation on inorganic crystal formation and stability.

The study of the mechanical properties of calcium carbonate biominerals has focused primarily on large specimens, such as shells, that can be easily subjected to conventional mechanical tests. There is a large number of studies on shells, which date back to the late 70s [4] and 80s [5]. A comprehensive tabulation is provided by Yang et al. [6]. The mechanical properties of shell or nacre still fascinate researchers, because of their excellent strength compared with mineral phase of calcium carbonate [6–9]. There is an unequivocal effect of the structure hierarchy and organic phase on mechanical properties of shells [10–14]. Different mechanisms for toughening have been proposed. For instance, the asperities in the tile surfaces have been proposed to be the major factor [15,16]. These mechanisms have been recently discussed and compared [17,18]. There have also been a more limited number of studies on pearls [19,20].

Since the size of otoliths in the carp grown in our laboratory is too small for conventional mechanical tests, their mechanical properties have not yet been reported. For this reason the current study focuses on nano and micro-indentation hardness. It was also the goal of this research to establish the effect of crystal polymorph on the mechanical response.

2. Experimental procedures

The laboratory-cultured fresh water carp (Fig. 1) was dissected and a pair of lapilli and asterisci were extracted. Because of the size and shape of sagittae, it was impossible to remove them (carp length of about 17 cm). The lapillus and asteriscus samples were then immersed in alcohol for 24 h for cleaning, and subsequently dried and stored. In order to eliminate effects from different samples, one lapillus and one asteriscus were used for nano-indentation, and the other lapillus and asteriscus from the same fish were used for micro-indentation,

The otolith samples were embedded in epoxy resin, ground with sand paper (#180 to #4000) with water, and then polished with Al_2O_3 (0.3 μm and 0.05 μm). During the polishing process, the microscope was used to observe the sample surface until a clear ring structure appeared in asteriscus sample (Fig. 2b).

The indentations were made along two directions, shown in Fig. 3(a): in Group 1, three indentation orientations are defined. Two lines were made in the ring structure zone, the indentations were

* Corresponding author.
E-mail address: biomater@mail.tsinghua.edu.cn (Q. Feng).

0928-4931/$ – see front matter © 2012 Elsevier B.V. All rights reserved.
http://dx.doi.org/10.1016/j.msec.2012.10.015

Fig. 1. Experimental materials: laboratory-cultured fresh water carp, body length of 17 cm; a pair of lapilli and a pair of asterisci.

made between the rings (Fig. 3a, lines 1 and 2); a third line was made between the ring zones, fully composed of calcium carbonate (Fig. 3a, line 3). This method was chosen to establish the effect of organic matrix (bright rings) on the nano-mechanical properties of asteriscus. In Group 2, an "indentation line" was made from the asteriscus core to the edge to compare the nano-mechanical properties of asteriscus in different positions (Fig. 3c, line 4). For the lapillus, the growth ring structure did not show after polish; hence, two "indentation lines" were made perpendicular to each other, both from the edge to the other end, both crossing the lapillus core (Fig. 3d, lines 5 and 6).

A CSM Instrument Nano-indentation Tester (NHTX S/N: 01-00005) with an indenter of Berkovich geometry (S/N B-L09) was used to perform the indentation tests. For the micro hardness tests, LECO M-400-H1 hardness testing machine was used [18]. The testing method was ASTM E384 micro hardness, (Vickers Hardness Test). A diamond cone with an apical angle of 136° was used; the loading force was 300 gf, about 2943 mN.

A field emission environmental scanning electron microscope (ESEM) was used to characterize the sample surface after indentation testing. The Phillips XL30 ESEM provides extremely high resolution (2 nm) images in high vacuum mode using the Secondary Electron detector at 30 kV, and the low kV imaging, down to 0.5 kV, allows the user to view very sensitive and delicate specimens.

3. Results and discussion

The growth ring structure can be seen after polishing the asteriscus sample. In Group 1, for all three orientations, the measured hardness and elastic modulus are fairly consistent (Fig. 5a). In Group 2, the hardness and modulus do not vary much from the core to edge (Fig. 5b), which indicates a fairly uniform distribution of composition and structure on asteriscus.

For the lapillus, the hardness and modulus did not vary much from one end to the core, then to the opposite end in lines 5 and 6 (Fig. 3d), which also showed a uniform composition of organic matrix and inorganic crystals of lapillus. Fig. 4 shows the load/displacement curves of asteriscus of Group 1 (Fig. 4a) and Group 2 (Fig. 4b), and lapillus (Fig. 4c). The load/displacement curves of each figure have the same shape and position, which means that the hardness and modulus (slope of the displacement curve of the maximum point) are similar. These results demonstrate the well-distributed calcium carbonate/organic matrix composition and hierarchical structure of lapillus and asteriscus.

Fig. 5(a) shows the comparison between nano- and micro-indentation hardness of lapillus and asteriscus. The abscissa is a normalized distance, since the spacing between micro-indentations is necessarily much larger than between nano-indentations. It can be seen that the nano-indentation of lapillus displays the highest value

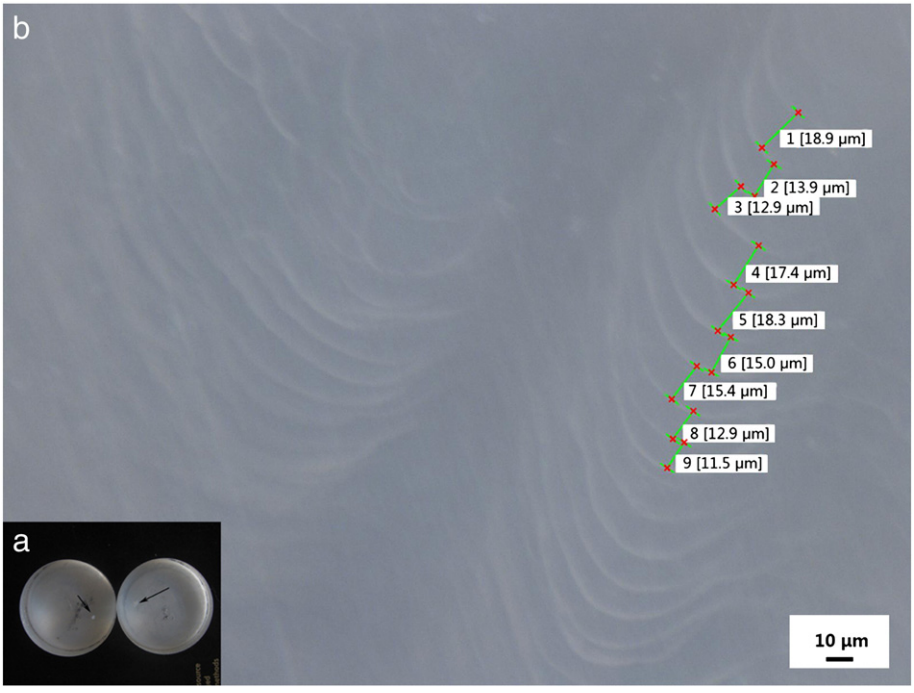

Fig. 2. Micrograph of asteriscus surface after polishing, showing the ring structure and spacing between them.

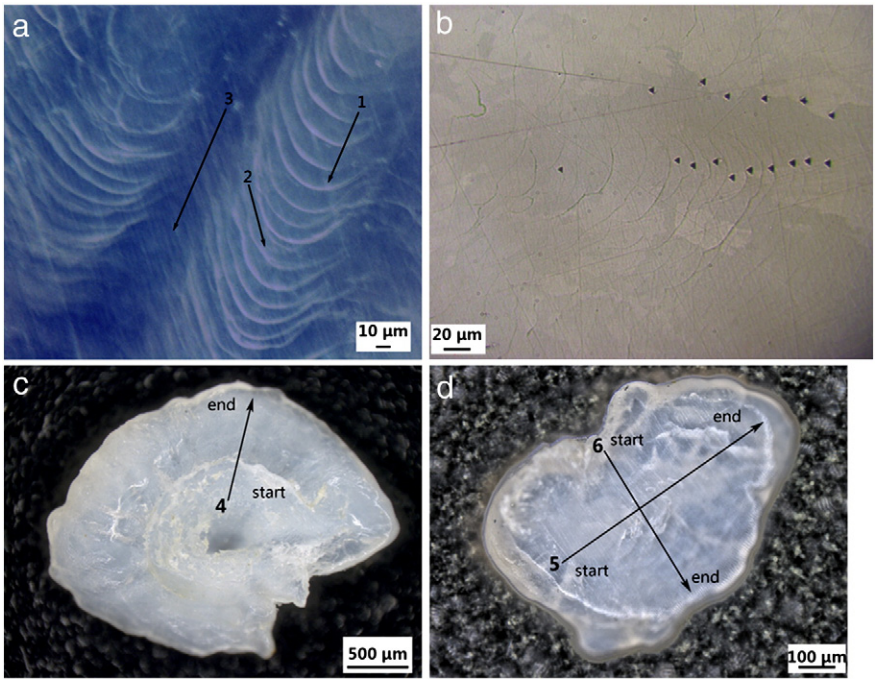

Fig. 3. a) Indentation lines of Group 1 on asteriscus: 1 and 2 within the ring structure region, 3 outside the ring structure region; b) nano-indentations of Group 1 on asteriscus; c) indentation direction of Group 2 on asteriscus (line 4); and d) nano-indentation lines 5 and 6 on lapillus.

of about 4.9 GPa. The nano-indentation hardness of asteriscus is significantly lower, about 3.2 GPa. Consistently, the micro-hardness of lapillus, about 2.8 GPa, is higher than that of asteriscus, about 2.2 GPa. The means and standard deviations are shown in Table 1. The nano-hardness is significantly higher than the micro hardness. This is consistent with other investigations and is connected to the scale of the indentation. Thus, fewer crystal defects affect the testing results in nano-indentation.

The elastic modulus and creep rate are plotted in Fig. 5(b) and (c), respectively. There is no systematic variation along the lines. The modulus is higher for lapillus because of the stronger bonding; the creep rate is lower and this is attributed to a smaller fraction of the organic phase. It is known that biopolymers are prone, due to their viscoelasticity, to creep and stress relaxation.

In the one-way ANOVA, the method of Least-Significant Difference (LSD), multiple comparisons (Table 2), the p-value of each group is less than 0.05, there are significant differences between each group. And for both the nano- and micro-hardness tests, the hardness and modulus of lapillus are higher than those of asteriscus, which is due to the different crystal polymorph.

Fig. 6a is the ESEM of a micro-indentation in lapillus; the surface maintains the shape of the quadrangular pyramid base, which is approximately 40 μm. Fig. 6b shows the ESEM figure of a microindentation in

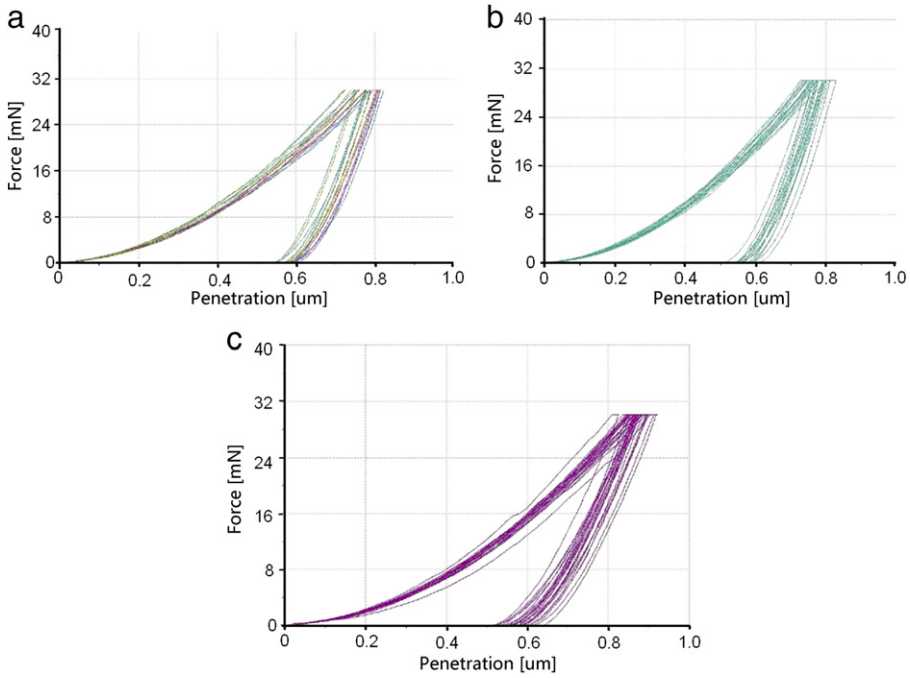

Fig. 4. Nanoindentation load-penetration curves on otoliths. a) asteriscus Group 1, purple for line 1, gold for line 2 and teal for line 3; b) asteriscus Group 2; and c) lapillus.

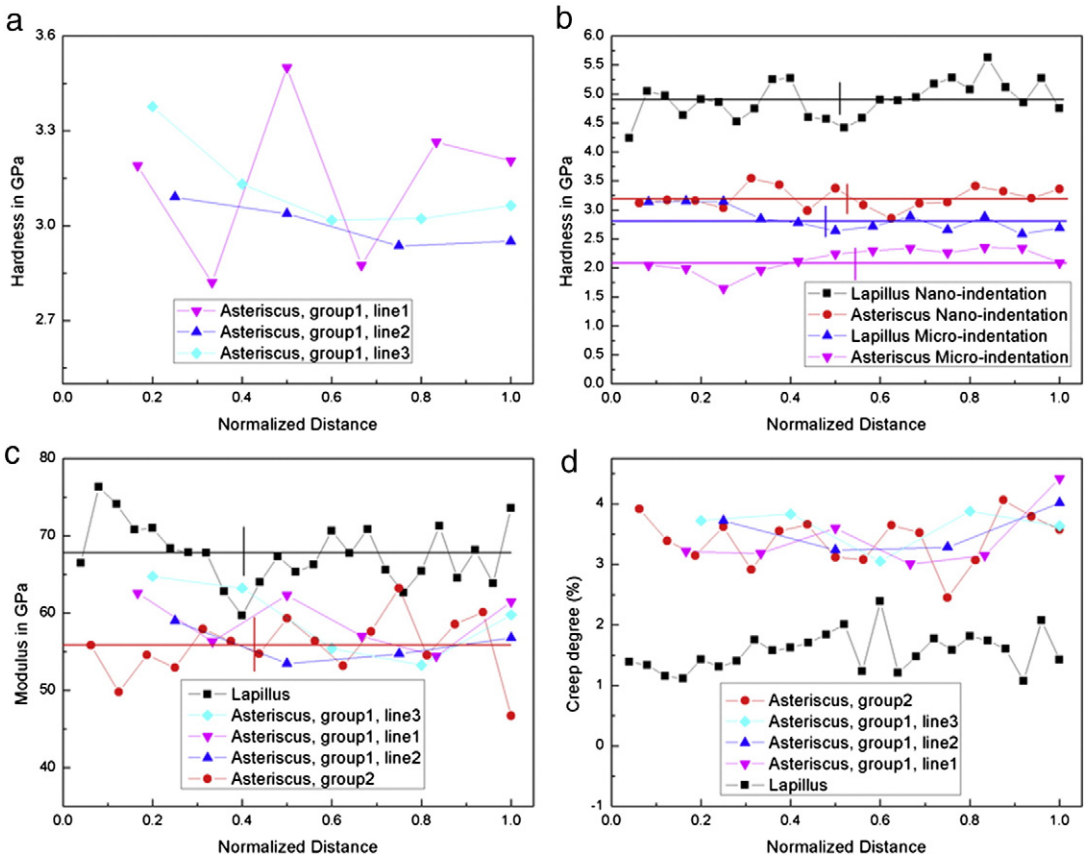

Fig. 5. (a) Nano-indentation hardness of asteriscus (Group 1, lines 1, 2 and 3); (b) comparison of hardness in micro- and nano-indentation of asteriscus (group 2) and lapillus (straight lines in the plot represent average value); (c) elastic modulus (from nano-indentation); and (d) extent of creep (from nano-indentation). The abscissa of the three plots represents a normalized distance.

Table 1
Hardness of lapillus and asteriscus in micro and nanoindentation tests.

	Lapillus	Asteriscus
Average microindentation hardness (GPa)	2.8	2.1
Standard deviation	0.196	0.201
Average nanoindentation hardness (GPa)	4.9	3.2
Standard deviation	0.322	0.185

asteriscus. Since this vaterite biomineral is more brittle, the shape of the tip is not maintained, and the size of the indentation is larger than that of lapillus, about 80 μm. Cracks extending from the indentation vertices show that both lapillus and asteriscus are brittle. The size of the micro-indentation (40 μm) is smaller than the size of a domain in the lapillus hierarchical structure, about 100 μm [2], if the indentation fell into a domain where all the "aragonite sticks" with a same orientation, the cracks have a tendency to form along the same direction with the sticks, as showed in Fig. 6a. The cracks emanating from points 1 and 3 are much

Table 2
Multiple comparisons.

ANOVA		Sum of squares	df	Mean square	F	Sig.
Between groups		662251.915	3	220,750.638	398.307	.000
Within groups		33807.555	61	554.222		
Total		696059.470	64			
LSD (I) VAR00001	(J) VAR00001	Mean difference (I–J)	Std. error	Sig.	95% confidence interval	
					Lower bound	Upper bound
Asteriscus micro	Lapillus micro	−65.12500*	9.61095	.000	−84.3433	−45.9067
	Asteriscus nano	−98.87940*	8.99022	.000	−116.8565	−80.9023
	Lapillus nano	−255.68013*	8.26765	.000	−272.2123	−239.1479
Lapillus micro	Asteriscus micro	65.12500*	9.61095	.000	45.9067	84.3433
	Asteriscus nano	−33.75440*	8.99022	.000	−51.7315	−15.7773
	Lapillus nano	−190.55513*	8.26765	.000	−207.0873	−174.0229
Asteriscus nano	Asteriscus micro	98.87940*	8.99022	.000	80.9023	116.8565
	Lapillus micro	33.75440*	8.99022	.000	15.7773	51.7315
	Lapillus nano	−156.80074*	7.53709	.000	−171.8721	−141.7294
Lapillus nano	Asteriscus micro	255.68013*	8.26765	.000	239.1479	272.2123
	Lapillus micro	190.55513*	8.26765	.000	174.0229	207.0873
	Asteriscus nano	156.80074*	7.53709	.000	141.7294	171.8721

* The mean difference is significant at the 0.05 level.

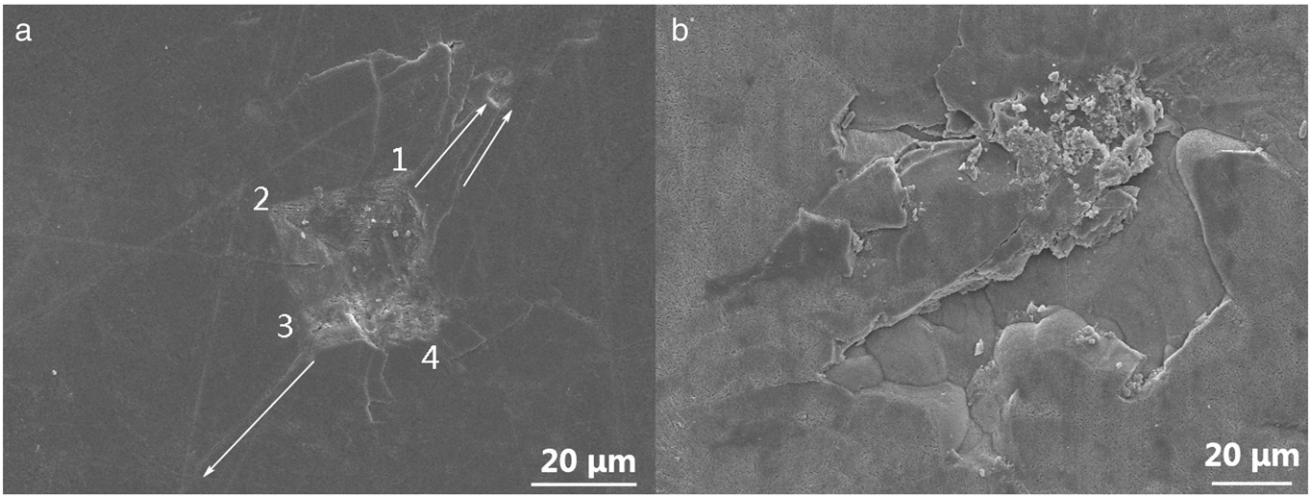

Fig. 6. ESEM micrographs of micro-indentations on otoliths. a) lapillus; and b) asteriscus.

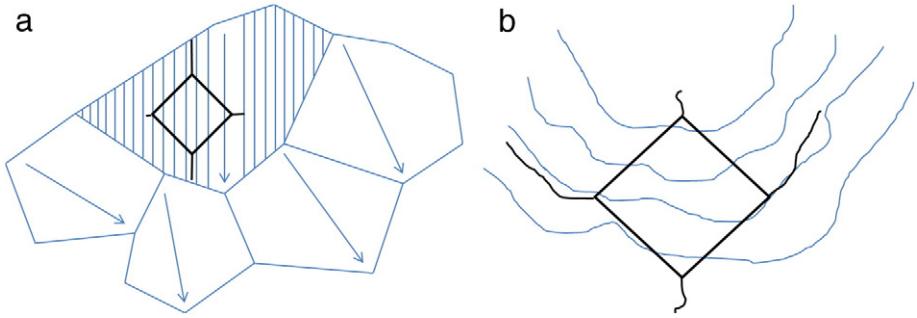

Fig. 7. Schematic representation of the cracks emanating from micro-indentations in otolith: a) lapillus; and b) asteriscus.

longer than those from points 2 and 4, in the perpendicular direction. The arrows in the figure point out the direction of the "aragonite crystals". In Fig. 2b, the measurement of the ring structure size in asteriscus, the average gap length of the rings is 15.14 ± 2.59 μm, the indentation crosses several rings on the surface; the irregular directions of the cracks may follow the directions of the rings. A schematic representation of the cracks is shown in Figs. 7a and b. Wen et al. also interpreted the cracks occurring after micro indentation in another biomineral: *Saxidomus purpuratus* shell [6].

The difference in Young's modulus and hardness can be rationalized on the basis of the structural differences. In lapillus, that is aragonitic, the structure is rhombic. The Ca^{2+} and CO_3^{2-} ions form in an alternate layered structure; these layers are perpendicular to the c-axis. The Ca^{2+} ions are hexagonal close packed, and the space between them is about 0.497 nm. The CO_3^{2-} triangle is parallel to the *ab*-face, similar to the structure of NaCl. However, in aragonite crystals the CO_3^{2-} group rotates 30°; so, some of the CO_3^{2-} ions rise 0.96 nm along the c-axis. Thus two kinds of CO_3^{2-} layers are formed, with different orientations.

In asteriscus, the inorganic $CaCO_3$ crystal is vaterite, which is the metastable phase of $CaCO_3$ belonging to the hexagonal system. The positions of CO_3^{2-} ions in the crystal are uncertain (disorder displacement); also the Ca^{2+} and CO_3^{2-} ions are not packed as closely as those in the aragonite crystals, and thus the mechanical properties of vaterites are not as high as aragonites [21].

4. Conclusions

The hardness of the of two carp otoliths, lapillus and asteriscus, was measured and compared. The asteriscus possesses rather consistent mechanical properties, with nano-indentation hardness around 3.2 GPa, and modulus close to 57 GPa, whereas the lapillus has a mean hardness of 4.9 GPa, and modulus of 67 GPa. The differences are due to the crystal structures of asteriscus (vaterite) and lapillus (aragonite). Both asteriscus and lapillus exhibit certain degree of creep, which indicates some time dependence of mechanical behavior due to the presence of organic interlayers.

Acknowledgment

The authors are grateful for the financial support from the National Natural Science Foundation of China (51072090, 51061130554) and Doctor Subject Foundation of the Ministry of Education of China (20100002110074). They thank Dr. Wen Yang for help in manuscript preparation.

References

[1] Z. Li, Q.L. Feng, Rare Metal Mater. Eng. 36 (2007) 47–49.
[2] Z. Li, Y.H. Gao, Q.L. Feng, Mater. Sci. Eng. C Biol. Sci. 29 (2009) 919–924.
[3] D.N. Ren, Y.F. Ma, Z. Li, Y.H. Gao, Q.L. Feng, J. Cryst. Growth 325 (2011) 46–51.
[4] J.D. Currey, Proc. R. Soc. Lond. B Biol. Sci. 196 (1977) 443–463.
[5] A.P. Jackson, J.F.V. Vincent, R.M. Turner, Proc. R. Soc. Lond. B Biol. Sci. 234 (1988) 415–440.
[6] W. Yang, G.P. Zhang, X.F. Zhu, X.W. Li, M.A. Meyers, J. Mech. Behav. Biomed. 4 (2011) 1514–1530.
[7] W. Yang, N. Kashani, X.W. Li, G.P. Zhang, M.A. Meyers, Mater. Sci. Eng. C Biol. Sci. 31 (2011) 724–729.
[8] P.Y. Chen, A.Y.M. Lin, Y.S. Lin, Y. Seki, A.G. Stokes, J. Peyras, E.A. Olevsky, M.A. Meyers, J. McKittrick, J. Mech. Behav. Biomed. 1 (2008) 208–226.
[9] F. Barthelat, C.M. Li, C. Comi, H.D. Espinosa, J. Mater. Res. 21 (2006) 1977–1986.
[10] F. Song, Y.L. Bai, J. Mater. Res. 18 (2003) 1741–1744.
[11] X.D. Li, W.C. Chang, Y.J. Chao, R.Z. Wang, M. Chang, Nano Lett. 4 (2004) 613–617.
[12] G. Mayer, M. Sarikaya, Exp. Mech. 42 (2002) 395–403.
[13] F. Barthelat, H. Tang, P.D. Zavattieri, C.M. Li, H.D. Espinpsa, J. Mech. Phys. Solids 55 (2007) 306–337.

[14] F. Song, A.K. Soh, Y.L. Bai, Biomaterials 24 (2003) 3623–3631.
[15] R.Z. Wang, Z. Suo, A.G. Evans, N. Yao, I.A. Aksay, J. Mater. Res. 16 (2001) 2485–2493.
[16] A.G. Evans, Z. Suo, R.Z. Wang, I.A. Aksay, M.Y. He, J.W. Hutchinson, J. Mater. Res. 16 (2001) 2475–2484.
[17] M.A. Meyers, P.Y. Chen, A.Y.M. Lin, Y. Seki, Prog. Mater. Sci. 53 (2008) 1–206.
[18] P.Y. Chen, J. McKittrick, M.A. Meyers, Prog. Mater. Sci. 57 (2012) 1492–1704.
[19] L. Qiao, Structure of Freshwater Vaterite Pearl and Its Biomineralization Mechanism (PhD thesis), Materials Science and Engineering Department, Tsinghua University, Beijing, 2008, pp. 113–120.
[20] L.E. Murr, D.A. Ramirez, JOM 64 (2012) 469–474.
[21] http://www.wmtr.com/Content/ASTME384.htm.